PHANTOM NODE METHOD FOR ARBITRARILY CRAKED PROBLEMS WITH 4-NODE QUADRILATERAL ELEMENTS

PHƯƠNG PHÁP NÚT ẢO CHO BÀI TOÁN CÓ VẾT NỨT BẤT KỲ ĐƯỢC RỜI RẠC BẰNG PHẦN TỬ TỨ GIÁC 4 NÚT

Chau Dinh Thanh[1,a], Le Viet Tuan[1,b], Nguyen Van Hieu[2,c], Goangseup Zi[3,d]
[1] Ho Chi Minh City University of Technology and Education
[2]Ho Chi Minh City University of Architecture
[3]School of Civil, Environmental and Architectural Engineering, Korea University

TÓM TẮT

Phương pháp nút ảo được phát triển để mô phỏng vết nứt bất kỳ trong các kết cấu được rời rạc bằng phần tử tứ giác 4 nút. Bằng cách chồng các phần tử tứ giác 4 nút tại vị trí vết nứt, phương pháp nút ảo có thể mô phỏng vết nứt không phụ thuộc vào lưới phần tử hữu hạn. Một quan hệ động học của các phần tử tứ giác 4 nút xếp chồng được phát triển mới giúp mô phỏng trường hợp mũi vết nứt nằm trong phần tử. Hệ số tập trung ứng của một số bài toán cơ bản có vết nứt được tính để kiểm tra độ chính xác của phương pháp nút ảo đề nghị. Sức mạnh và hiệu quả của phương pháp nút ảo khi mô phỏng vết nứt bất kỳ không phụ thuộc lưới phần tử hữu hạn được minh họa bằng các ví dụ tính toán sự phát triển vết nứt do tải trọng mỏi.

Từ khóa*: phương pháp nút ảo, phần tử tứ giác 4 nút, vết nứt, hệ số tập trung ứng suất (SIFs), mỏi.*

ABSTRACT

A phantom node method is developed for problems discretized by 4-node quadrilateral elements to describe arbitrary cracks. By overlapping elements at the position of the crack, the method may treat cracks independently of the mesh. The tip of the crack can be located inside the element owing to development of a new kinematic relation between overlapped 4-node quadrilateral elements. Stress intensity factors (SIFs) of several benchmark problems containing cracks are computed to verify the proposed method. The robustness and efficiency of the method when used to model arbitrary cracks are also demonstrated by solving some crack propagation examples.

Keywords*: phantom-node method, 4-node quadrilateral elements, cracks, SIFs, fatigue.*

I. INTRODUCTION

During working engineering structures usually appear cracks due to material failures, inappropriate calculations of strength and/or fatigue strength, overloads or other unpredictable problems. Such damage generally causes huge costs for repair and maintenance. So that, the analysis of such cracked structures plays an important role in designing and maintaining of many engineering applications.

To analyze components or structures containing cracks, the analytical or numerical approaches can be used. In which, the analytical solutions have been derived only for cracked problems with relatively simple geometry and boundary conditions. In contrast, to deal with real-life problems with arbitrary cracks, complicated shape and general boundary conditions the numerical methods have been applied. In general, the numerical methods can be divided into three main classes based on displacement

approximation and discretized techniques of the problem domain, called finite element methods (FEM), boundary element methods or mesh less methods. Among these groups, the FEM [1] is one of the most popular methods to analyze cracked structures. However, the requirement of the mesh topology aligned with the geometry of the crack imposes a challenge of remeshing on the FEM when modeling crack propagation. To overcome the time-consuming remeshing with minor modification of the FEM technique the extended finite element methods (XFEM) [2] have been developed and successfully applied for two/three dimensional and plate/shell structures containing cracks.

Recently, based on the idea of Hansbo and Hansbo[3] an alternative approach, called the phantom-node method, has been coined to describe the crack independently of the FEM mesh topology without using discontinuous displacement approximations as in the XFEM. The phantom-node method which duplicates homologous nodes to build overlapping paired elements for the case of the tip of the crack strictly located on the edges of elements has been implemented in the FEM codes with for two/three dimension[4,5]or shell structures[6].

To consider the case in which the tip of the crack can be placed inside of an element, Rabczuk*et al.*[7] has developed kinematic constrains for the three-node triangular and four-node quadrilateral overlapping pair elements containing the crack tip. The idea of the kinematic constrains for the overlapping pair elements in[7] has been successfully extended to the cracked shell structures discretized by the MITC3 degenerated shell elements [8].

In this paper, the kinematic relations between the homologous phantom nodes of the four-node quadrilateral elements are deeply described to model the crack tip inside an element following the brief presentation in [7]. The accuracy and robustness of the proposed formulation in computing stress intensity factors (SIFs) and modeling the crack propagation independently from the mesh topology are investigated.

The paper is outlined as follows. In the next section, the phantom-node method with kinematic constrains for four-node quadrilateral elements is derived. The equilibrium equations and numerical integration of the stiffness matrices are presented in section 3. Numerical examples are illustrated in section 4. The last section draws some conclusions.

II. THE PHANTOM-NODE METHOD FOR 4-NODE QUADRILATERAL ELEMENTS

Consider a 2-dimensional cracked body discretized by four-node quadrilateral elements. Due to the crack, the finite elements of the discretization can be divided into uncracked, cracked and tip elements. In the following subsections, the displacement approximations of each type of elements are described in details.

1. The uncracked elements

The uncracked elements which are not cut by the crack are the standard iso parametric 4-node quadrilateral finite elements. The displacement fields are approximated by [9]

$$\mathbf{u}(\xi,\eta)=\sum_{I=1}^{4}N_I(\xi,\eta)\mathbf{u}_I \tag{1}$$

Here, $\mathbf{u}=\{u,v\}^T$ are the displacement approximations in the *x*-, *y*-directions of the Cartesian coordinates; $\mathbf{u}_I=\{u_I,v_I\}^T$ are the displacements at node *I*; and $N_I(\xi,\eta)$ are the standard bilinear shape functions.

2. The cracked elements

When elements, namely cracked elements, are totally cut by a crack, the displacement fields are continuous on each part of the elements but discontinuous across the crack.

In other words, the displacement fields of the cracked elements can be combination of two separate displacement fields each of which is continuous within its own part [3]. To describe the continuity of the each part or the discontinuity across the crack the real nodes of the cracked element are duplicated to create phantom nodes. The phantom nodes and the real nodes then build two overlapping paired complete finite elements and the displacement fields of which can be approximated by the standard finite element approximation.

In the case of a 4-node quadrilateral element completely intersected by a crack, there are two different positions of a crack in relation to the edges of a cracked element as shown in Figure 1. The Figure 1 also indicates the phantom nodes, which are hollow circles, and the two overlapping paired elementsΩ_e^+ and Ω_e^-.

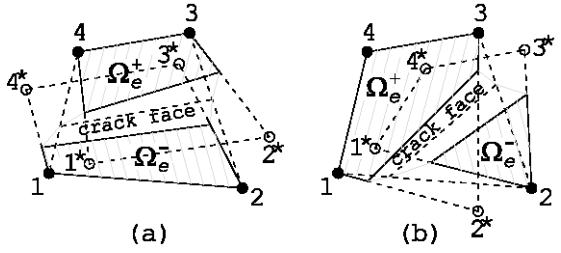

Figure 1. Overlapping paired elements for a cracked element.

The standard approximation given in Eq. is now applied on each part of the cracked element. Hence, the displacement fields of the cracked element can be written as follows

$$\mathbf{u}_{cr}(\xi,\eta)=\begin{cases}\sum_{J=1}^{4} N_J(\xi,\eta)\mathbf{u}_J & \text{in } \Omega_e^+\\ \sum_{K=1}^{4} N_K(\xi,\eta)\mathbf{u}_K & \text{in } \Omega_e^-\end{cases}$$

Wherein, $J\in\{1^*,2^*,3,4\}$, $K\in\{1,2,3^*,4^*\}$ for Figure 1a and $J\in\{1,2^*,3,4\}$, $K\in\{1^*,2,3^*,4^*\}$ for Figure 1b.

3. The tip elements

To a tip element, which is partially cut by a crack, the displacement field is discontinuous across the crack but continuous at the tip of the crack and the remains of the element. Particularly, the displacement field near the tip is high gradient [10]and no jump at the tip. To consider the high gradient displacement field in vicinity of the tip the XFEM adds branch functions which are basic functions of the analytical displacements[2,11]. However, we do not know many branch functions due to only few analytical solutions of fracture mechanics problems known. Moreover, the branch functions can increase computational complexity but not efficiently improve the accuracy, especially in case of using assumed strain techniques[7,8,12]in the XFEM. Some researches[13, 14] have been shown that the high gradient displacements in the vicinity of the tip can be successfully modeled by using refinement of the mesh, in spite of large increase in the computational effort. And notice that in all cases there is no crack-opening displacement at the tip.

Base on the characteristics of the displacement field in a tip element, Rabczuk*et al* [7] have built kinematic constrains for the overlapping elements so that the crack opening displacement vanished at the tip of the crack. It also means that the high gradient displacement near the crack tip is not described to accelerate the convergent rate of numerical solutions. Especially, in the case of the linear elastic fracture mechanics (LEFM), the asymptotic displacement field around the crack tip is treated by fine meshing. Honestly, it is very difficult to integrate high gradient functions into the phantom-node method.

A 4-node quadrilateral tip element for the phantom-node method is here explained and derived in more details from [7]. Consider a case in which a crack cuts edge 12 and the tip is located inside the element, see Figure 2. Due to the discontinuity across the crack, the displacements of node 1 and node 2 must

belong to two separate displacement fields approximated by the standard FEM. In addition, the vanishing of crack opening displacement at the crack tip leads to the displacements of node 3 and node 4 independent from the displacement approximations of node 1 and node 2. To fulfill the standard finite element approximations for these three different displacements phantom nodes are added at the identical location of the real nodes.

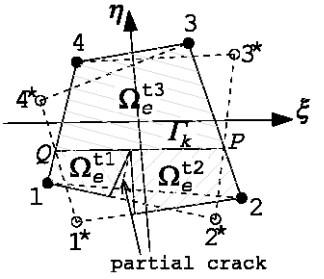

Figure 2.Overlapping triple elements and kinematic constrains for a tip element

However, to guarantee the continuity of the tip element except the partial crack the three separate displacements of node 1, node 2, and node 3 and node 4 have to be constrained to represent common displacement fields between them. In the bilinear standard displacement fields of a 4-node quadrilateral element, the identical displacements of the three separate displacement approximations is only a straight line through the crack tip and parallel to one of the axes of the parent coordinates [7] such as line Γ_k in Figure 2.

Therefore, the displacements of node 1 are described by element 12^*3^*4 in which nodes 2^* and 3^* are respectively the phantom nodes of the real nodes 2 and 3. Similarly, element 1^*234^* represents the displacements of node 2 and element 1234 for the displacements of nodes 3 and 4. In addition, the identical displacements of these three elements along the line Γ_k lead to the following kinematic constrains between the phantom nodes.

From the similar triangles $\Delta 2P2^*$ and $\Delta 3P3^*$, one has

$$\frac{\mathbf{u}_3^* - \mathbf{u}_3}{\mathbf{u}_2 - \mathbf{u}_2^*} = \frac{1-\eta_P}{1+\eta_P} = k \tag{3}$$

where $\mathbf{u}_3^*$ is displacements of phantom node 3^* and η_P is the η- parent coordinate of point P, see Figure 2.

From the Eq., the displacements of phantom node 3 are constrained by

$$\mathbf{u}_3^* = k\mathbf{u}_2 - k\mathbf{u}_2^* + \mathbf{u}_3 \tag{4}$$

Or the displacements of overlapping element 12^*3^*4 are constrained by

$$\begin{Bmatrix} \mathbf{u}_1 \\ \mathbf{u}_2^* \\ \mathbf{u}_3^* \\ \mathbf{u}_4 \end{Bmatrix} = \underbrace{\begin{bmatrix} \mathbf{I} & \mathbf{0} & \mathbf{0} & \mathbf{0} & \mathbf{0} & \mathbf{0} \\ \mathbf{0} & \mathbf{0} & \mathbf{0} & \mathbf{0} & \mathbf{0} & \mathbf{I} \\ \mathbf{0} & k\mathbf{I} & \mathbf{I} & \mathbf{0} & \mathbf{0} & -k\mathbf{I} \\ \mathbf{0} & \mathbf{0} & \mathbf{0} & \mathbf{I} & \mathbf{0} & \mathbf{0} \end{bmatrix}}_{\mathbf{T}_1} \underbrace{\begin{Bmatrix} \mathbf{u}_1 \\ \mathbf{u}_2 \\ \mathbf{u}_3 \\ \mathbf{u}_4 \\ \mathbf{u}_1^* \\ \mathbf{u}_2^* \end{Bmatrix}}_{\mathbf{u}_e^t} \tag{5}$$

Here, $\mathbf{I}$ and $\mathbf{0}$ are unit and zero matrices of dimensions 2x2, respectively.

To build the kinematic constrains for overlapping element 1^*234^* consider the similarity of triangles $\Delta 1Q1^*$ and $D4Q4^*$, one can write

$$\frac{\mathbf{u}_4^* - \mathbf{u}_4}{\mathbf{u}_1 - \mathbf{u}_1^*} = \frac{1-\eta_Q}{1+\eta_Q} = k \Rightarrow \mathbf{u}_4^* = \mathbf{u}_4 + k\mathbf{u}_1 - k\mathbf{u}_1^*$$

withη_Q is the η- parent coordinate of point Q and η_Q=η_P. Or the nodal displacement constrains of element $1^*234^*$are

$$\begin{Bmatrix} \mathbf{u}_1^* \\ \mathbf{u}_2 \\ \mathbf{u}_3 \\ \mathbf{u}_4^* \end{Bmatrix} = \underbrace{\begin{bmatrix} \mathbf{0} & \mathbf{0} & \mathbf{0} & \mathbf{0} & \mathbf{I} & \mathbf{0} \\ \mathbf{0} & \mathbf{I} & \mathbf{0} & \mathbf{0} & \mathbf{0} & \mathbf{0} \\ \mathbf{0} & \mathbf{0} & \mathbf{I} & \mathbf{0} & \mathbf{0} & \mathbf{0} \\ k\mathbf{I} & \mathbf{0} & \mathbf{0} & \mathbf{I} & -k\mathbf{I} & \mathbf{0} \end{bmatrix}}_{\mathbf{T}_2} \underbrace{\begin{Bmatrix} \mathbf{u}_1 \\ \mathbf{u}_2 \\ \mathbf{u}_3 \\ \mathbf{u}_4 \\ \mathbf{u}_1^* \\ \mathbf{u}_2^* \end{Bmatrix}}_{\mathbf{u}_e^t} \tag{6}$$

As a result, in the case of the partial crack through edge 12 as demonstrated in Figure 2the tip element for the phantom-node method of 4-node quadrilateral elements is modeled by

overlapping triple elements and the constrains given by Eqs. and .

By the same above approach, one can constructs overlapping triple elements and corresponding kinematic constrains for the three other cases where the partial crack sequentially passes across edge 23, 34 and 41.

III. EQUATIONS OF EQUILIBRIUM

Let Ω be a 2-dimensional body containing a crack Γ_{cr} free of tractions. The body boundary G is imposed by prescribed displacements on the necessary boundary Γ_u and tractions $\boldsymbol{t}_0$ on the natural boundary $\Gamma_t$in which $\Gamma_u \cup \Gamma_t = \Gamma$and$\Gamma_u \cap \Gamma_t = 0$. Assume that the strains and displacements are small and materials work in linear elastic range.

The domain Ω is discretized by 4-node quadrilateral elements Ω_e. Following the standard finite element procedure, the discretized equilibrium equations of the body Ω can be obtained as

$$\mathbf{f}_{\text{int}} = \mathbf{f}_{ext} \tag{7}$$

Herein, the internal force

$$\mathbf{f}_{\text{int}} = \sum_{\substack{uncracked\\elements}} \int_{\Omega_e} \mathbf{B}^T\mathbf{D}\mathbf{B}\mathrm{d}\Omega\mathbf{u}_e + \sum_{\substack{cracked\\elements}} \left(\int_{\Omega_e^+} \mathbf{B}^T\mathbf{D}\mathbf{B}\mathrm{d}\Omega\mathbf{u}_e^{cr+} + \int_{\Omega_e^-} \mathbf{B}^T\mathbf{D}\mathbf{B}\mathrm{d}\Omega\mathbf{u}_e^{cr-} \right) + \sum_{\substack{tip\\elements}} \left(\int_{\Omega_e^{t1}} \mathbf{T}_1^T\mathbf{B}^T\mathbf{D}\mathbf{B}\mathbf{T}_1\mathrm{d}\Omega\mathbf{u}_e^t + \int_{\Omega_e^{t2}} \mathbf{T}_2^T\mathbf{B}^T\mathbf{D}\mathbf{B}\mathbf{T}_2\mathrm{d}\Omega\mathbf{u}_e^t + \int_{\Omega_e^{t3}} \mathbf{B}^T\mathbf{D}\mathbf{B}\mathrm{d}\Omega\mathbf{u}_e \right)$$

and the external force $\mathbf{f}_{ext} = \sum_{\substack{all\\element}} \int_{\Gamma_e} \mathbf{N}^T\mathbf{t}_0\mathrm{d}\Gamma$

in which **B** is the strain-displacement matrix; **D** is plane strain or plane stress constitutive matrix; $\mathbf{u}_e$ is nodal displacements of an uncracked element; $\mathbf{u}_e^{cr+}$ and $\mathbf{u}_e^{cr-}$ are respectively nodal displacements of the overlapping paired elements for a cracked element; and $\mathbf{u}_e^t$is nodal displacements of a tip element plus the phantom nodes of the edge cut by the partial crack, see Eqs. and .

In this paper, the numerical Gaussian integration is employed. To overlapping elements, their domains belonging to the cracked body (hatched areas in Figure 1 and Figure 2) are divided into subtriangles and the standard Gaussian integration is mapped into these subtriangles [2] to compute the internal force because overlapping elements are realized on the physical domains only.

IV. NUMERICAL VERIFICATION

To evaluate the accuracy and robustness of the presented method, we compute SIFs of two benchmark problems and predict crack propagation due to fatigue loads without remeshing. In following examples, the domain forms of the interaction integrals [2] are employed to compute the SIFs.

1. Calculation of SIFs

Given a plane stress plate of 1 thickness with dimensions and applied loads as shown in Figure 3. The material has Young modulus $3\text{x}10^7$ and Poisson's ratio 0.25.

The analytical SIF of the opening mode for the plate under tension is given in [2] as

$$K_I = F\left(\frac{a}{b}\right)\sigma\sqrt{\pi a}$$

with

$$F\left(\frac{a}{b}\right) = 1.12 - 0.231\left(\frac{a}{b}\right) + 10.55\left(\frac{a}{b}\right)^2 - 21.72\left(\frac{a}{b}\right)^3 + 30.39\left(\frac{a}{b}\right)^4$$

When sustained the shear the SIF values of the opening mode K_I=34.0 and shearing mode K_{II}=4.55computed by [15] are used as references.

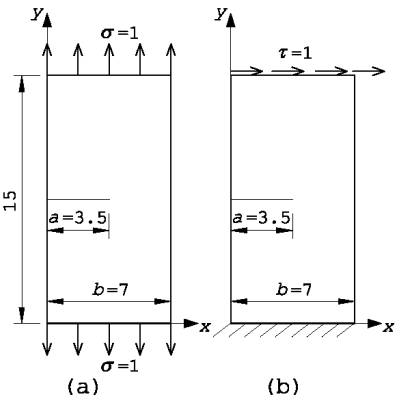

Figure 3. Edge cracked plate under (a) tension and (b) shear.

The plate is discretized by n_xxn_y 4-node quadrilateral elements, in which n_x and n_y are number of elements along the x and y axes, respectively. Three structural meshes, 15x33, 45x99, 75x165 elements, are used to compare the accuracy and the convergent rate of the presented method with the phantom-node method for 3-node triangular elements and the XFEM for 4-node quadrilateral elements. The normalized SIFs, which are numerical results divided by the above reference results, are shown in Figure 4 for the plate under the tension, and Figure 5 and Figure 6when the plate is sustained the shear.

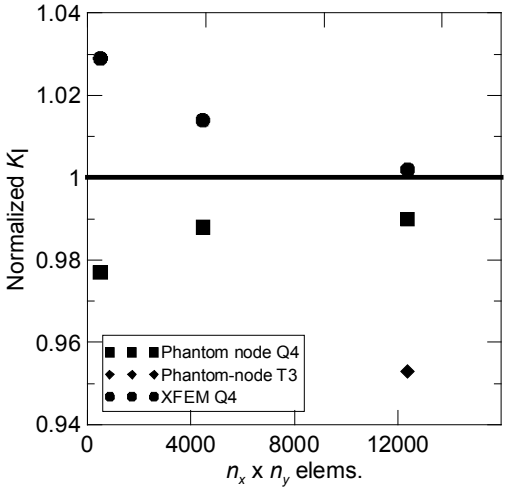

Figure 4.Normalized K_I for the edge cracked plate under tension.

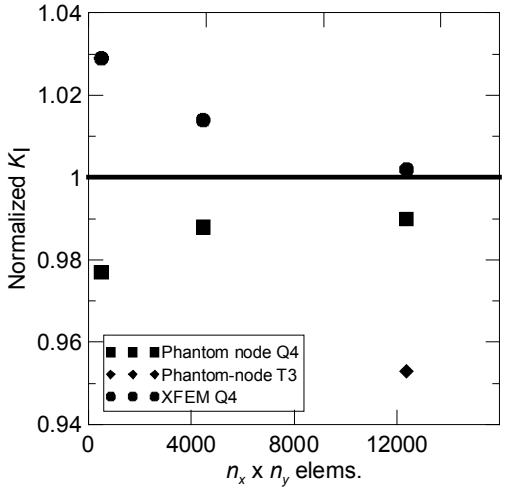

Figure 5. Normalized K_I for the edge cracked plate under shear.

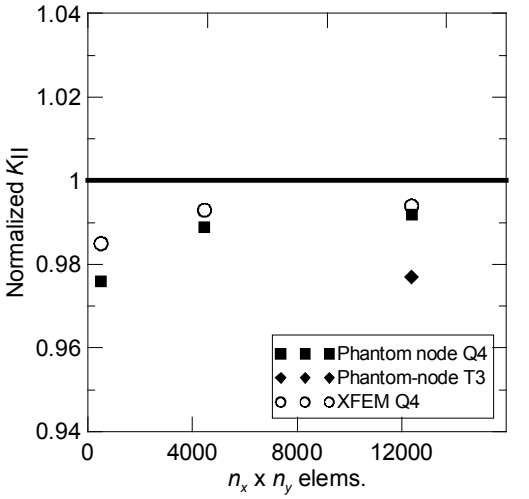

Figure 6. Normalized K_{II} for the edge cracked plate under shear.

The numerical results indicate that as the mesh density increases the computed SIFs of the presented method approach the reference results. And, the phantom-node method for 4-node quadrilateral elements gives the great improvement in accuracy as compared with the phantom-node method for 3-node triangular elements. However, the presented method cannot capture the accuracy and the convergent rate of the XFEM which employs the asymptotic displacement approximation.

2. Prediction of fatigue life

In this section, the efficient use of the presented method to simulate crack growth without remeshing is demonstrated. The development of an edge angled crack in a 2-dimensional plate under constant cyclic fatigue loads as in [16] is simulated. The plate is a 100 mm x 200 mm rectangle having a 20 mm initial crack inclined an angle of 40^0 with a line perpendicular to edges subjected to a cyclic tension ranging from σ_{min}=0 to σ_{max} = 40 N/mm, see Figure 7a. The elastic material properties are Young modulus E = 74000 N/mm2; Possion's ratio n = 0.3. In this paper, the fatigue crack propagation follows the Paris' law [17] with the fatigue properties C = 2.087136x10^{-13},m = 3.32 and fracture toughness K_{IC} = 1897.36 N/$mm^{3/2}$.

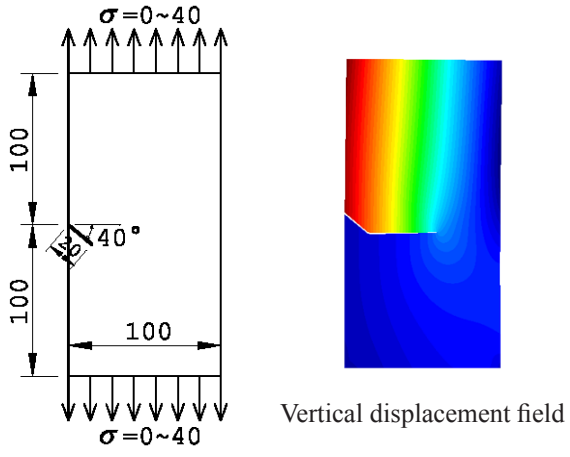

Figure 7. (a) Dimensions and an initial crack of the plate; (b) Profile of the crack growth.

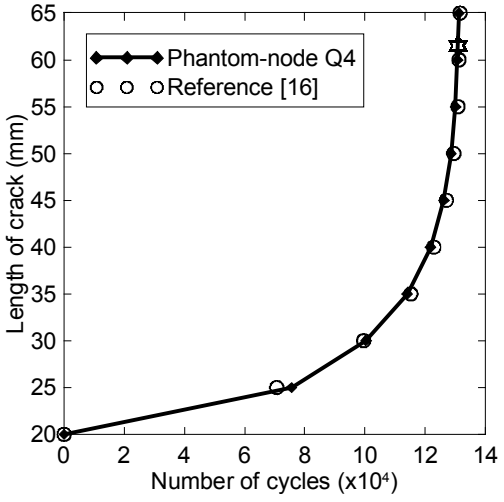

Figure 8. Fatigue life of the cracked plate.

The plate is discretized by12880 four-node quadrilateral elements in which there are 80 elements in the horizontal edge and 161 elements in the vertical edge. In this paper, crack growth is simulated by successive linear increments of 5-mm length and the direction determined by the maximum circumferential stress criterion [2]. The stable crack growth stops when the equivalent SIF reaches the fracture toughness. As a result, the fatigue life of the structure is 130920 cycles corresponding to the crack length of 61.5 mm and the crack growth profile is illustrated in Figure 7b. The curves in Figure 8demonstrate the relation between number of cycles and crack length during the crack propagation with the star mark presenting the failure. The **Figure 8** indicates the very good agreement between the present method and [16] which employs the messless method.

V. CONCLUSION

The phantom-node method with kinematic constrains for overlapping four-node quadrilateral elements describing a crack tip located inside an element was introduced. The present method permits an arbitrary crack mostly independent from mesh topology. The SIF results of some benchmark problems showed the more accuracy of the present method than those using the phantom-node method for three-node triangle elements. The method was also applied to simulate the fatigue crack propagation of 40^0-edge cracked plate without remeshing and gave similar results to other references. These result in the reliability of the present method to simulate and compute structures with cracks.

ACKNOWLEDGEMENTS

The last author appreciates the New & Renewable Energy Core Technology Program of the Korea Institute of Energy Technology Evaluation and Planning (KETEP) for a research grant from the Ministry of Trade, Industry & Energy, Republic of Korea, (No. 20133010021770) to Korea University.

REFERENCES

[1] R. S. Barsoum, On the use of isoparametric finite elements in linear fracture mechanics, *International Journal for Numerical Methods in Engineering*, 10, pp. 25–37, 1976.

[2] N. Moes, J. Dolbow, and T. Belytschko, A finite element method for crack growth without remeshing, *International Journal for Numerical Methods in Engineering*, 46, pp. 131–150, 1999.

[3] A. Hansbo and P. Hansbo, A finite element method for the simulation of strong and weak discontinuities in solid mechanics, *Computer Methods in Applied Mechanics and Engineering*, 193, pp. 3523–3540, 2004.

[4] J. Mergheim, E. Kuhl, and P. Steinmann, A finite element method for the computational modelling of cohesive cracks, *International Journal for Numerical Methods in Engineering*, 63, pp. 276–289, 2005.

[5] J. Mergheim, E. Kuhl, and P. Steinmann, Towards the algorithmic treatment of 3D strong discontinuities, *International Journal for Numerical Methods in Engineering*, 23, pp. 97–108, 2007.

[6] P. M. A. Areias, J. H. Song, and T. Belytschko, Analysis of fracture in thin shells by overlapping paired elements, *Computer Methods in Applied Mechanics and Engineering*, 195, pp. 5343–5360, 2006.

[7] T. Rabczuk, G. Zi, A. Gerstenberger, and W. A. Wall, A new crack tip element for the phantom-node method with arbitrary cohesive cracks, *International Journal for Numerical Methods in Engineering*, 75, pp. 577–599, 2008.

[8] T. Chau-Dinh, G. Zi, P.-S. Lee, T. Rabczuk, and J.-H. Song, Phantom-node method for shell models with arbitrary cracks, *Computers and Structures*, 92–93, pp. 242–256, 2013.

[9] K.-J. Bathe, *Finite Element Procedures*. Prentice Hall International, Inc., 1996.

[10] T.-P. Fries and T. Belytschko, The extended/generalized finite element method: An overview of the method and its applications, *International Journal for Numerical Methods in Engineering*, 84, pp. 253–304, 2010.

[11] A. Asadpoure and S. Mohammadi, Developing new enrichment functions for crack simulation in orthotropic media by the extended finite element method, *International Journal for Numerical Methods in Engineering*, 69, pp. 2150–2172, 2007.

[12] J. Dolbow, N. Moes, and T. Belytschko, Modeling fracture in Mindlin-Reissner plates with the extended finite element method, *International Journal of Solids and Structures*, 37, pp. 7161–7183, 2000.

[13] H. Nguyen-Dang and N. Tran-Thanh, Analysis of cracked plates and shells using ‘metis’ finite element model, *Finite Elements in Analysis and Design*, 40, pp. 855–878, 2004.

[14] C. H. Furukawa, M. L. Bucalem, and I. J. G. Mazella, On the finite element modeling of fatigue crack growth in pressurized cylindrical shells, *International Journal of Fatigue*, 31, pp. 629–635, 2009.

[15] J. F. Yau, S. S. Wang, and H. T. Corten, A mixed-mode crack analysis of isotropic solids using conservation laws of elasticity, *Journal of Applied Mechanics*, 47, pp. 335–341, 1980.

[16] M. Duflot and H. Nguyen-Dang, A meshless method with enriched weight functions for fatigue crack growth, *International Journal for Numerical Methods in Engineering*, 59, pp. 1945–1961, 2004.

[17] P. C. Paris and F. Erdogan, A critical analysis of crack propagation laws, *Journal of Basic Engineering*, 85, pp. 528–534, 1963.